LOW-DIMENSIONAL DYNAMICS FOR THE COMPLEX GINZBURG–LANDAU EQUATION

J.D. RODRIGUEZ and L. SIROVICH
*Center for Fluid Mechanics and the Division of Applied Mathematics, Brown University, P.O. Box 1966,
Providence, RI 02912, USA*

A method is presented which results in low-dimensional dynamical systems for situations in which low-dimensional attractors are known to exist. The method is based on the use of the Karhunen–Loeve procedure for the determination of an *optimal* basis and the subsequent use of the Galerkin procedure to generate the dynamical system. The method is applied to two problems for the Ginzburg–Landau equation for which large databases have been obtained. In each instance a dynamical system is generated which has roughly twice the number of degrees of freedom as the Hausdorff dimension of the exact case. It is also demonstrated that the approximations are robust in that they are accurate over a wide range of parameter space.

1. Introduction

In a number of applications it has been well established that dissipation acts to diminish the dimension of the set to which a given system is attracted [1–3]. Typically one is confronted with a system described by partial differential equations and thus requiring an infinite number of dimensions for its description, but for which from other considerations one knows that the (chaotic) attractor is not only finite but also of relatively small dimension. An example is furnished by the Ginzburg–Landau (GL) equation,

$$G(A) = A_t - q^2(\mathrm{i} + c_0) A_{xx} - \rho A$$

$$- (\mathrm{i} - \rho) A|A|^2$$

$$= 0. \qquad (1.1)$$

This equation for the complex-valued amplitude A incorporates the mechanisms of linear growth, non-linearity and dispersion. See the preceding paper [4] (hereafter referred to as I) for further details and references. In I we consider the Neumann and Dirichlet problems for (1.1). The attractor in each instance as measured by its Lyapunov dimension [5], d_L, was small, $d_L(\max) = 3.06$ for the first case and a reference value was $d_L = 9.1$, in the second case.

The usual theory and calculations accompanying estimates of attractor dimension, d_L, do not furnish any practical means for reducing the dynamical description of such systems. A method, not immediately related to the dimension estimates, which does substantially reduce the order of the dynamical study has recently been presented [6]. In that report it was shown that the GL equation for the Neumann attractor, which has a maximal dimension $d_L \approx 3.06$, can be reduced to a system of three complex differential equations. In addition the same system of six equations accurately describes the GL equation over a wide parameter range even though the dynamical system was derived for a single parameter value, $q = 0.95$. In the present paper we furnish some additional details for that case and in addition

present an analogous treatment of the Dirichlet case. This second case is one in which spatial as well as temporal chaos plays a role.

The method of approach is based on the Karhunen–Loeve (KL) [7, 8] procedure, which also plays a role in fluid turbulence [9, 10], and other chaotic problems [11]. Briefly stated, the KL procedure generates an optimal system of basis functions, based on second-order statistics. These *best* fitting functions are then used in a Galerkin approximation to the GL equation. Since the KL basis functions are derived for a specific set of parameter values, an important question is the range of accuracy of the derived dynamical system. This, as we show, is substantial in both instances.

We begin with a brief review and summary of the KL procedure with particular attention to the role it plays in the types of problems under investigation.

2. Derivation of the near ideal basis

The *flow* $A(x, t)$ is assumed to be chaotic and the system sufficiently *aged* so that the system point moves on the chaotic attractor. We denote by

$$\{ A_n(x) \} = \{ A(x, t_n) \} \tag{2.1}$$

an ensemble of *snapshots* of the flow at uncorrelated times $\{ t_n \}$. The ensemble of states (2.1) is supposed to be large enough so that the attractor is sufficiently sampled so that we can perform the necessary statistics. Since solutions to (1.1) are invariant under multiplication by complex numbers lying on the unit circle,

$$G(A) = 0 \Rightarrow G(e^{ic}A) = 0 \tag{2.2}$$

for c real, it follows from averaging over this group of transformations that

$$\langle A \rangle = 0. \tag{2.3}$$

The angular brackets in (2.3) and in what follows denote an ensemble average.

A *geometry* is introduced into the space through the complex inner product

$$(u, v) = \int \bar{u}(x) \, v(x) \, dx, \tag{2.4}$$

where the integration is over the interval which in our case is $(0, \pi)$. We seek the maximum of the most likely state on the chaotic attractor, ϕ, defined by

$$\lambda = \max \langle |(\phi, A)|^2 \rangle, \tag{2.5}$$

subject to the normalizing condition

$$(\phi, \phi) = E = \langle (A, A) \rangle. \tag{2.6}$$

E is the average *energy* of the system and condition (2.6) requires that ϕ lies on the *sphere* nearest which the system point moves, on the average.

The solution to this problem is given by the principle eigenfunction of the kernel

$$K(x, y) = \langle A(x, t) \, \bar{A}(y, t) \rangle, \tag{2.7}$$

which is just the two-point correlation function. $K(x, y)$ regarded as a kernel is easily seen to be Hermitian, non-negative, and square integrable. It then follows from Mercer's theorem [12] that the eigenfunctions $\{ \phi_n \}$,

$$\int K(x, y) \, \phi_n(y) \, dy = K\phi_n = \lambda_n \phi_n, \tag{2.8}$$

form a complete orthonormal set such that

$$K = \sum_{n=1}^{\infty} \lambda_n \phi_n(x) \, \bar{\phi}_n(y). \tag{2.9}$$

While ϕ_1 solves the problem posed by (2.5) and (2.6), ϕ_k solves the same problem subject to the additional side condition that $(\phi_k, \phi_m) = 0$ for $m < k$. The content of the above discussion, along with the statement that

$$A = \sum a_n(t) \, \phi_n(x), \quad a_m = (\phi_n, A) \tag{2.10}$$

almost everywhere is known as the Karhunen–Loeve theorem [13].

Some additional properties of this procedure bear mention. Since

$$\lambda_n = (\phi_n, K) = \langle |(\phi_n, A)|^2 \rangle$$

$$= \lim_{T \uparrow \infty} \frac{1}{T} |(\phi_n, A)|^2 \, dt, \qquad (2.11)$$

an eigenvalue λ_n can be regarded as measuring the mean energy of motion projected along the corresponding *direction*, ϕ_n. The mean energy, E, of the flow is

$$E = \int \langle A(x) \, \overline{A}(x) \rangle \, dx$$

$$= T_r K = \sum_n \lambda_n. \qquad (2.12)$$

3. Dynamical equations

The eigenfunctions discussed in section 2 can now be used to generate a dynamical system from the GL equation (1.1). To this end we express the solution in the form

$$A(x, t) = \sum_n a_n(t) \, \phi_n(x), \qquad (3.1)$$

where the ϕ_n are the eigenmodes derived from the Karhunen–Loeve decomposition. This is used in a Galerkin procedure [14], i.e. we project (3.1) and the GL equation onto a subset of the eigenmodes. This yields the modal equations,

$$\left(\phi_m, G \left(\sum_{n=1}^{N} a_n(t) \, \phi(x) \right) \right) = 0,$$

$$m = 1, \ldots, N. \qquad (3.2)$$

The eigenfunctions, $\{\phi_n\}$, are assumed to be ordered according to descending values of the eigenvalues, $\{\lambda_n\}$. Other criteria are of course possible.

Table 1
Eigenvalues for the Neumann problem at $q = 0.95$.

i	1	2	3
λ_i	0.8599	0.1380	0.2108×10^{-2}

It is worth noting in passing that the system (3.2) appears to differ in general form from what would be generated from the Navier–Stokes equations. In the latter case only a quadratic nonlinearity arises (from the *streaming* operator). Although not immediately apparent a Galerkin approximation to the Navier–Stokes equations also generates cubic non-linearities. The cubic terms are *unveiled*, when convective and advective terms are expressed in terms of the mean flow quantities. The latter are themselves quadratic functionals, and the net contribution is cubic. This has been observed by Aubry et al. [15] for the channel flow and also for Rayleigh–Bénard convection [16–18].

4. Neumann problem

For the full simulation of the Neumann problem given in I at $q = 0.95$ we obtain the eigenvalues in table 1. Below the third eigenvalue the mean energy is insignificant and by choosing a three-mode approximation we capture over 99% of the average energy of the system. If the first three complex eigenfunctions (which correspond to six real dimensions) are used in the Galerkin procedure outlined in section 3 we obtain the system of equations displayed in the appendix.

Poincaré plots and power spectra for the exact and three-mode solutions at $q = 0.95$ are shown in plate I. Inspection shows these to be virtually indistinguishable. The remaining panels in plate I show a selection of exact and approximate results. Of special note is the period doubling bifurcation which is captured to five significant places. For the range considered by us

$$0.6 \leq q \leq 1.3, \qquad (4.1)$$

the agreement between exact and approximate results is extremely close. The value of the transition points near the period-doubling sequence is the most significant discrepancy, see I. For the exact solution a transition occurs at 0.827, versus 0.84 for the three-mode approximation, a difference of 1.6%. For other values of q the variation is well under 1% (I). To compare the attractor for the reduced system to that of the full system we calculate the Lyapunov dimension for each case. For the Neumann problem the Lyapunov dimension was found by Keefe [19] to have a value of 3.047. The corresponding value calculated for the three-mode approximating system is 3.049.

In fig. 1 we show the surface $A(x, t)$ calculated from the three-mode calculation at $q = 0.95$, which should be compared with the exact results given in I. Since we are dealing with a chaotic regime, *sensitivity to small changes* should be expected. Thus in passing from the GL equation to the three-mode equations we affect such a small change. The resulting alteration in the solution can be seen in the comparison of the curves at the end of the simulation. Nevertheless as we have seen in the discussion thus far, the statistics of the two simulations are virtually identical. In summary we see that, although the equations presented in the appendix are derived for $q = 0.95$ they are *robust* in that they accurately predict the behavior encountered over the extended range (4.1).

From the spatial power spectrum shown in ref. [19] and the near sinusoidal nature of the eigenfunctions shown there, one might contemplate using purely sinusoidal modes. This is straightforward and gives an adequate description over the range (4.1). This has also been shown by Doelman [20], who made a detailed study of low-order sinusoidal truncations of the GL equation. However, this is not as accurate as three-mode theory in predicting transitions and of more importance it fails, for example, as c_0 in (1.1) is varied. The three-mode theory is more robust and continues to be accurate for a range of values of the parameters c_0 and ρ.
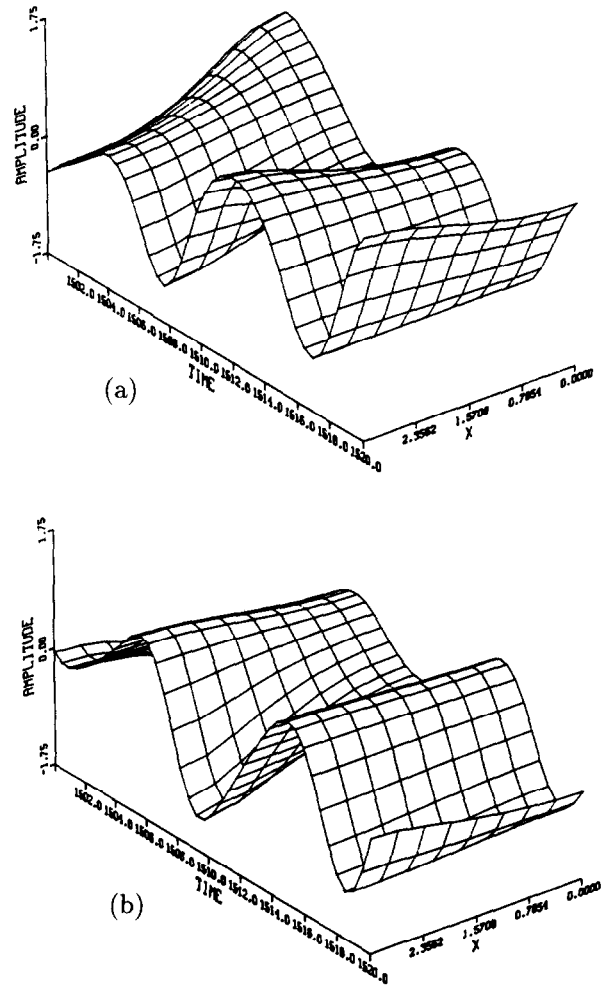

Fig. 1. Time history (20 time units); (a) three-mode solution (real part), (b) three-mode solution) (imaginary part).

5. Dirichlet problem

The first twelve eigenvalues for the Dirichlet problem are shown in table 2. In contrast to the previous case the magnitudes of the eigenvalues decrease more slowly. To bring out the relevant features we have normalized the eigenvalues so that their sum is equal to unity. Thus each eigenvalue is a probability that represents the percentage of energy of the system. Inspection of table 2 shows that choosing ten eigenvalues enables us to capture over 99% of the energy of the system, which was the criterion used for the Neumann

Table 2
The first twelve eigenvalues for the Dirichlet problem.

i	λ_i	i	λ_i
1	0.2602	7	0.2903×10^{-1}
2	0.1997	8	0.1349×10^{-1}
3	0.1870	9	0.7469×10^{-2}
4	0.1334	10	0.3810×10^{-2}
5	0.1110	11	0.2212×10^{-2}
6	0.4987×10^{-1}	12	0.1194×10^{-2}

problem and we have taken a ten-mode (or twenty-dimensional) approximation to treat this case. The first four eigenfunctions are displayed in fig. 2. The spatial structure of the solution for this case is considerably richer than in the Neumann case [6].

Since chaos for the Dirichlet boundary value problem occurs in a continuous band (I), with monotonically increasing d_L, the choice of value of q at which to perform the KL decomposition becomes arbitrary. Since machine demand becomes a factor we choose q equal to 0.14 as the nominal case. At this value of q, the Lyapunov dimension was calculated to be 9.088. This value is not a global maximum, and the dimension increases without bound as q continues to decrease. From this calculation we expect to capture the behavior of solutions at larger values of q and hope to also obtain a good approximation for smaller values of q. The Lyapunov dimension was computed to be 9.16 for the ten-mode approximation solution, an error of only a fraction 1%.
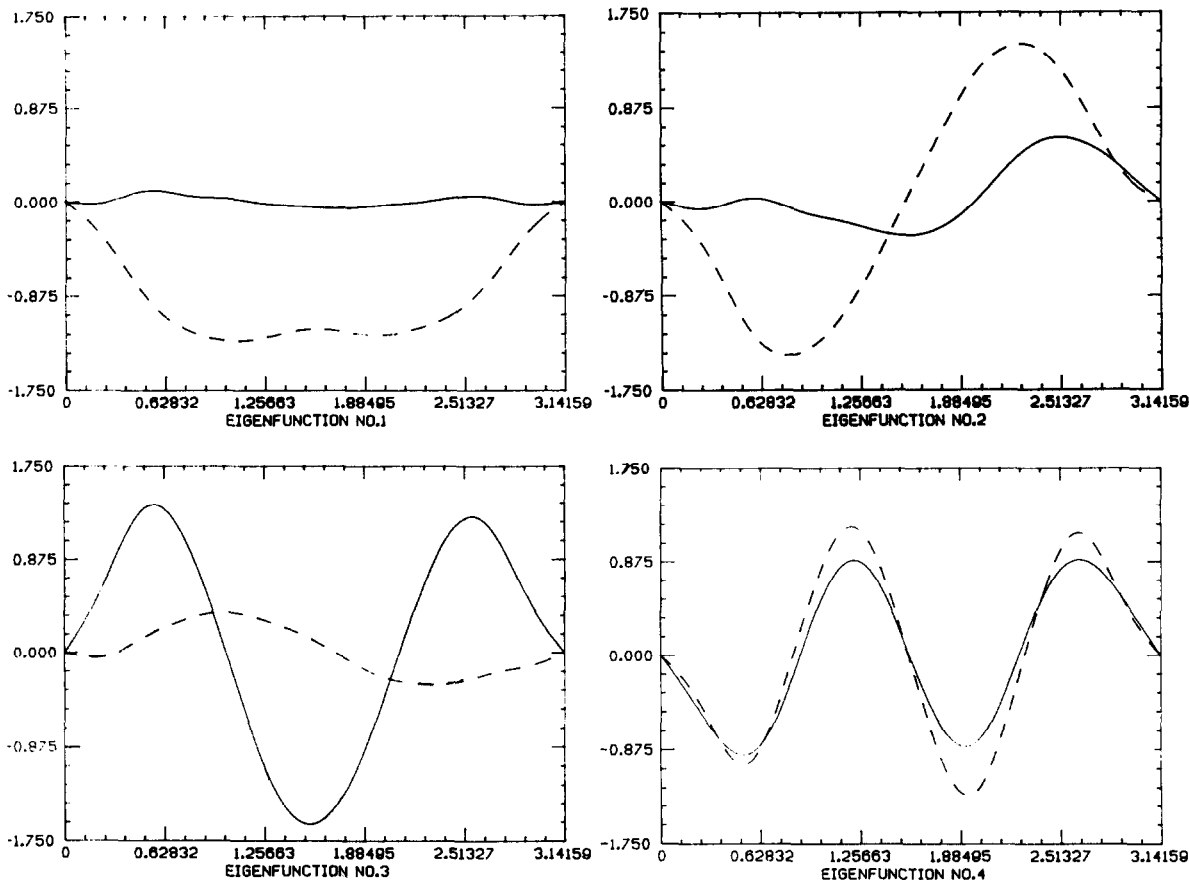

Fig. 2. Eigenfunctions, Dirichlet boundary value problem; (solid lines) real part, (dashed lines) imaginary part. Eigenfunctions 1 through 4 correspond to (a) through (d), respectively.
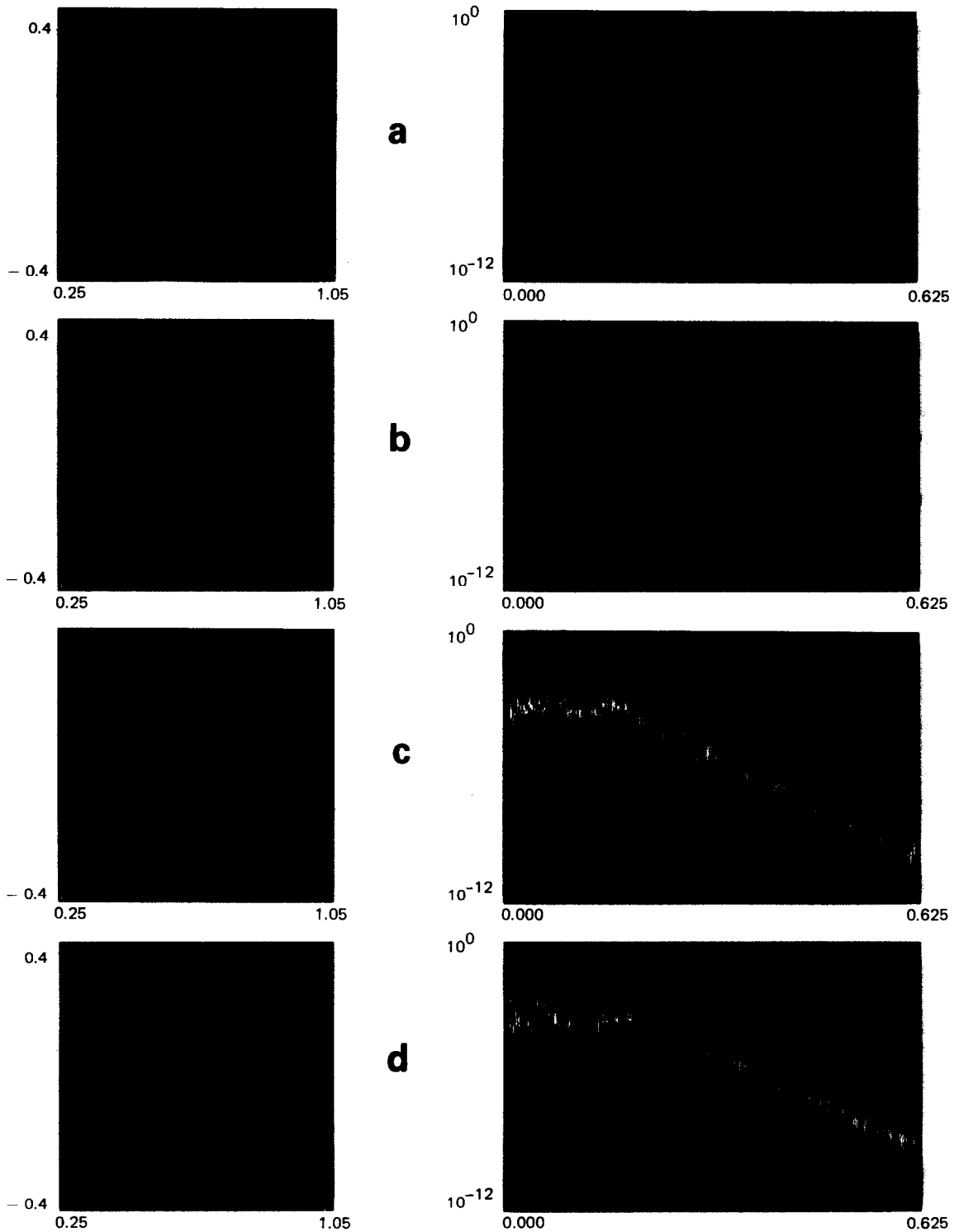
Plate I. 3-mode versus exact Ginzburg–Landau theory. Poincaré sections appear at the left and corresponding power spectra at the right. Yellow marks 3-mode and red exact GL theory – overlap appears white. (a) $q = 1.075$, (b) $q = 1.074$, (c) $q = 0.95$, (d) $q = 0.88$.
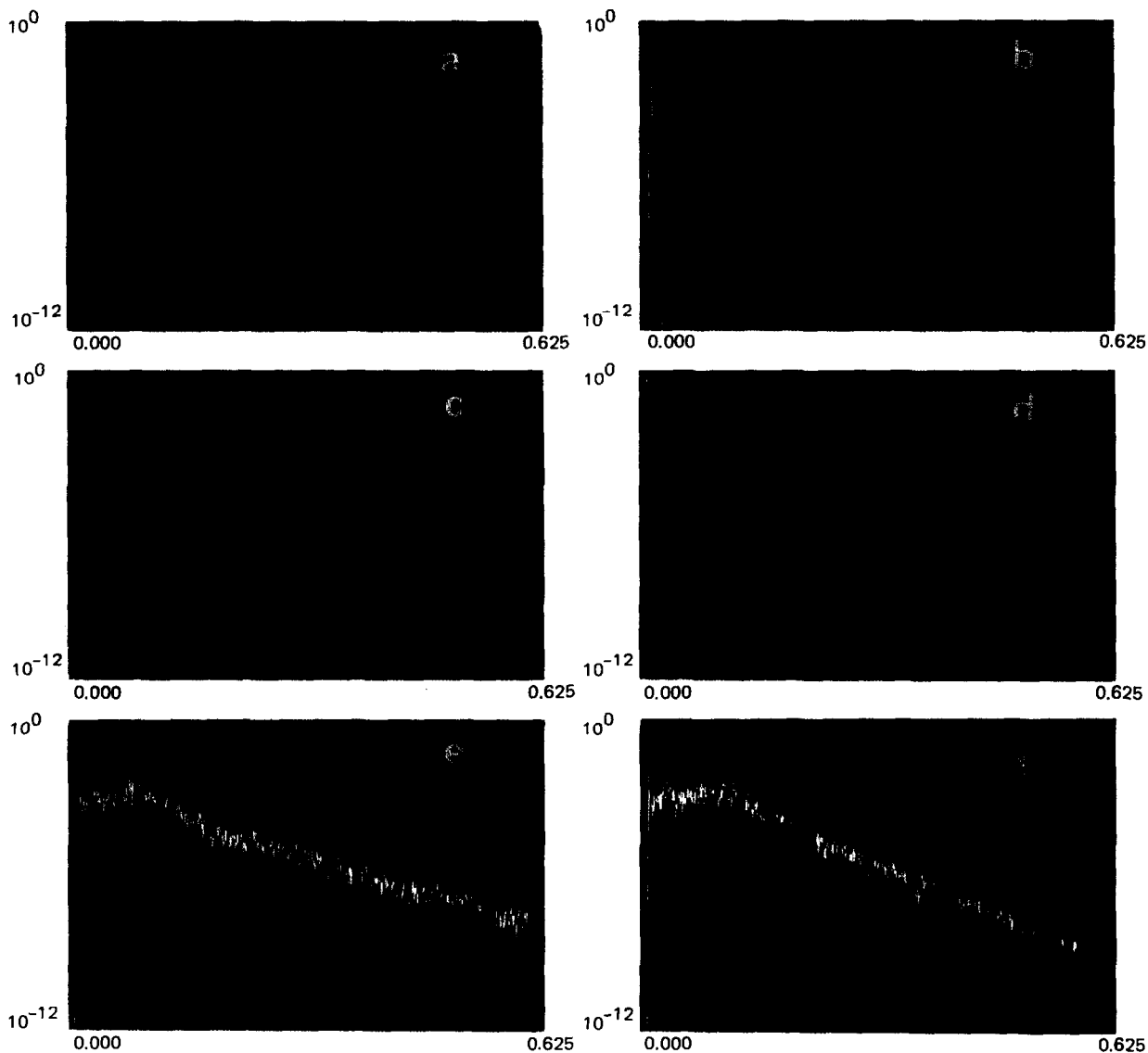
Plate II. 10-mode versus exact Ginzburg–Landau theory. The power spectra shown follow the color coding used in plate I. (a) $q=0.35$, (b) $q=0.27$, (c) $q=0.24$, (d) $q=0.23$, (e) $q=0.14$, (f) $q=0.08$.
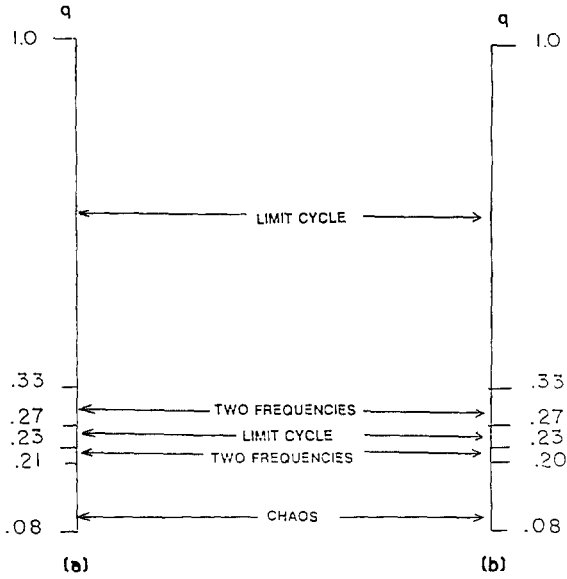
Fig. 3. Comparison of behavior, sticky boundary value problem.

(a)

(b)

Fig. 4. Time history (20 time units); (a) ten-mode solution (real part), (b) ten-mode solution (imaginary part).

Plots of the power spectra are shown for the exact solution and for the ten-mode solution in plate II. As in the three-mode approximation the agreement between the plots is excellent. Now again we wish to determine the accuracy of the reduced system over a range of parameter values.

A summary comparison of the exact and approximate solutions, as q varies, is shown in fig. 3. Again the qualitative behavior is virtually identical to the exact solution. In addition the values at the transition points are, if anything, in even better agreement than for the Neumann case. Note that for this case the parameter q has an even wider range than in the Neumann case. Subtleties of solution behavior such as the fact that even solution harmonics vanish are also mirrored in the ten-mode approximating system. The robustness of the approximation can be seen in the fact that the level of agreement with the pseudo spectral exact solution remains good even when smaller values of q are considered than the value of 0.14, at which the solution was derived. A comparison of power spectrum plots at $q = 0.08$ on plate II shows the approximation to be still in close agree-
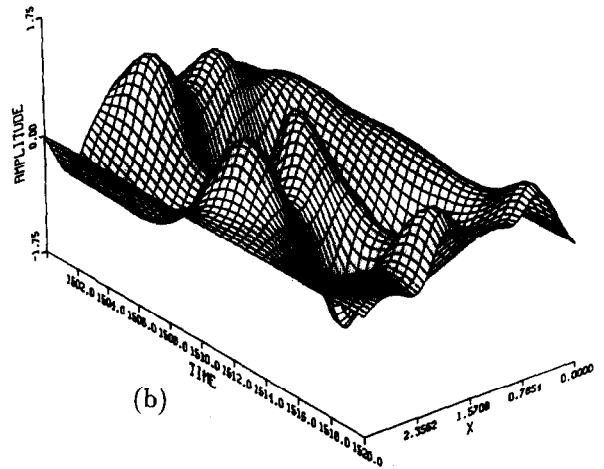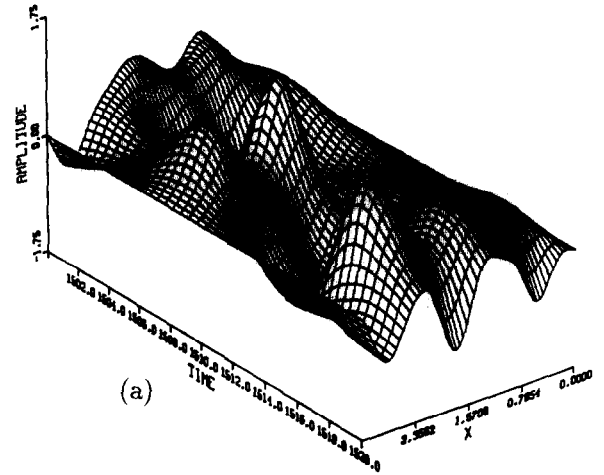
ment with the exact solution. In view of the extreme singularity of the $q = 0$ limit this is particularly noteworthy. Power spectra at other representative values of q are shown in plate II.

In fig. 4 we exhibit the surface $A(x, t)$ as calculated by the ten-mode simulation. This should be compared to the like figures in I. The suggestion of spatial chaos is clear in these figures. The remarks about sensitive dependence made at the end of section 4 again apply.

6. Conclusion

In summary, the above results indicate that significant simplifications of problem complexity can be realized by a proper choice of basis. By using the Karhunen–Loeve decomposition, to derive a basis set for a chaotic attractor, we were able to reduce the problem to such an extent that gains in computational time of two orders of magnitude were realized. This feature can be of great utility if an extensive parameter exploration is contemplated. Our deliberations suggest that one *muscular* calculation need to be carried out in order to derive a reduced set via the KL method coupled with a Galerkin procedure. The reduced system is then used for exploration in parameter space. For example on an IBM 3090, the integration of the three-mode system required approximately 70 s of CPU time, versus 600 s for the corresponding pseudo spectral solution. For the ten-mode system the run time was 700 s for a time history of 1500 time units, the pseudo spectral solution required 6000 s of CPU to generate the same time history. Thus we obtain a tenfold reduction in CPU time while the behavior of the reduced systems approximated the exact behavior closely over a wide parameter range.

Appendix

The equations for the three-mode approximations are:

$$
\begin{aligned}
\dot{A}_0 = {} & -q^2(0.00171 + 0.00684i)\,A_0 + 0.250A_0 - q^2(0.0414 + 0.166i)\,A_2 \\
& + (-0.251 + 1.00i)\,A_0|A_0|^2 + (-0.104 + 0.0682i)\,A_2|A_0|^2 \\
& + (-0.522 + 2.09i)\,A_0|A_1|^2 + (0.0301 + 0.0547i)\,A_0^2 A_2^* \\
& + (-0.500 + 2.00i)\,A_0|A_2|^2 + (-1.075 + 0.0565i)\,A_1^2 A_0^* \\
& + (-1.284 + 0.838i)\,A_2|A_1|^2 + (-0.525 + 0.559i)\,A_1^2 A_2^* \\
& + (-1.017 - 0.174i)\,A_2^2 A_0^* + (-0.0254 + 0.0258i)\,A_2|A_2|^2,
\end{aligned}
$$

$$
\begin{aligned}
\dot{A}_1 = {} & -q^2(0.251 + 1.006i)\,A_1 + 0.250A_1 + (-0.522 + 2.09i)\,A_1|A_0|^2 \\
& + (0.922 + 0.556i)\,A_1^* A_0^2 + (0.400 + 1.480i)\,A_0 A_1^* A_2 \\
& + (0.740 + 1.344i)\,A_0 A_1 A_2^* + (-1.284 + 0.838i)\,A_1 A_0^* A_2 \\
& + (-0.388 + 1.553i)\,A_1|A_1|^2 + (-0.510 + 2.042i)\,A_1|A_2|^2 \\
& + (-0.472 + 0.940i)\,A_2^2 A_1^*,
\end{aligned}
$$

$$
\begin{aligned}
\dot{A}_2 = {} & -q^2(0.0414 + 0.166i)\,A_0 + 0.250A_2 - q^2(1.003 + 4.011i)\,A_2 \\
& + (0.031 + 0.0547i)\,A_0|A_0|^2 + (-0.500 + 2.00i)\,A_2|A_0|^2 \\
& + (0.740 + 1.344i)\,A_0|A_1|^2 + (0.979 + 0.325i)\,A_0^2 A_2^* \\
& + (0.0205 + 0.0694i)\,A_0|A_2|^2 + (-0.525 + 0.559i)\,A_1^2 A_0^* \\
& + (-0.510 + 2.042i)\,|A_1|^2 A_2 + (-0.0261 + 1.052i)\,A_1^2 A_2^* \\
& + (-0.0254 + 0.0258i)\,A_2^2 A_0^* + (-0.375 + 1.500i)\,A_2|A_2|^2.
\end{aligned}
$$

References

[1] A. Brandstater, J. Swift, H.L. Swinney, H.L. Wolf, D. Farmer, E. Jen and P. Crutchfield, Low-dimensional chaos in a hydrodynamic system, Phys. Rev. Lett. 51 (1983) 1442.

[2] H.L. Swinney and J.P. Gollub, J. Fluid Mech. 94 (1979) 103.

[3] B. Malraison, P. Atten, P. Berge and M. Dubois, Dimension d'attracteurs étranges: une détermination expérimentale au régime chaotique de deux systèmes convectifs, Compt. Rend. Acad. Sci. (Paris) C297 (1983) 209.

[4] L. Sirovich, L. Rodriguez and B. Knight, Two boundary value problems for the Ginzberg–Landau equation, Physica D 43 (1990) 63–76.

[5] J. Kaplan and J. Yorke, Chaotic behavior in multi-dimensional difference equations, in: Springer Lecture Notes in Mathematics, Vol. 730 (Springer, Berlin, 1980) p. 228.

[6] L. Sirovich and J.D. Rodriguez, Coherent structures and chaos: a model problem, Phys. Lett. A 120 (1987) 211.

[7] K. Karhunen Ann. Acad. Sci. Fenn. Ser. A1 (1946) 37.

[8] M.M. Loeve, Probability Theory (Van Nostrand, Princeton, 1955).

[9] J.L. Lumley, Atmospheric Turbulence and Radio Wave Propagation (Nauka, Moscow, 1967).

[10] J.L. Lumley, Stochastic Tools in Turbulence (Academic Press, New York, 1970).

[11] D.S. Broomhead and G.P. King, Extracting qualitative dynamics from experimental data, Physica D 20 (1986) 217–236.

[12] F. Riesz and B. Sz. Nagy, Functional Analysis (Ungar, New York, 1955).

[13] R.B. Ash and M.F. Gardner, Topics in Stochastic Processes (Academic Press, New York, 1975).

[14] L.V. Kantorovich and V.I. Krylov, Approximate Methods of Higher Analysis (Interscience, New York, 1958).

[15] N. Aubrey, P. Holmes, J.L. Lumley and E. Stone, The dynamics of coherent structures in the wall region of turbulent boundary layer, J. Fluid Mech. 192 (1988) 115–175.

[16] L. Sirovich, H. Tarman and M. Maxey, An eigenfunction analysis of turbulent thermal convection, ed. B.E. Launder (Springer, Berlin, 1988).

[17] L. Sirovich, Chaotic dynamics of coherent structures, Physica D 37 (1989) 126–145.

[18] L. Sirovich and C. Sirovich, How dimensional description of complicated phenomena, Contemp. Math. 99 (1989) 277–305.

[19] L. Keefe, Dynamics of perturbed wavetrain solutions to the Ginzburg–Landau equation, Stud. Appl. Math. 73 (1985) 91.

[20] A. Doelman, Low dimensional truncated models of the Ginzburg–Landau equation, Prep. 18, Department of Mathematics, University of Utrecht (1988).